


## RESEARCH ARTICLE

The genomic landscape of estrogen receptor  $\alpha$  binding sites in mouse mammary glandMurugesan Palaniappan<sup>1</sup> <sup>1aa\*</sup>, Loc Nguyen<sup>1</sup>, Sandra L. Grimm<sup>1</sup>, Yuanxin Xi<sup>2ab</sup>, Zheng Xia<sup>2ac</sup>, Wei Li<sup>2</sup>, Cristian Coarfa<sup>3,4</sup>

**1** Department of Molecular and Cellular Biology, Baylor College of Medicine, Houston, United States of America, **2** Division of Biostatistics, Dan L. Duncan Cancer Center, Baylor College of Medicine, Houston, United States of America, **3** Dan L. Duncan Cancer Center, Baylor College of Medicine, Houston, United States of America, **4** Advanced Technology Core, Baylor College of Medicine, Houston, United States of America

<sup>aa</sup> Current address: Department of Pathology & Immunology and Center for Drug Discovery, Baylor College of Medicine, One Baylor Plaza, Houston, United States of America

<sup>ab</sup> Current address: Department of Bioinformatics and Computational Biology, The University of Texas MD Anderson Cancer Center, Houston, United States of America

<sup>ac</sup> Current address: Department of Molecular Microbiology & Immunology, Oregon Health & Science University, Portland, United States of America

\* [palaniap@bcm.edu](mailto:palaniap@bcm.edu)


 OPEN ACCESS

**Citation:** Palaniappan M, Nguyen L, Grimm SL, Xi Y, Xia Z, Li W, et al. (2019) The genomic landscape of estrogen receptor  $\alpha$  binding sites in mouse mammary gland. PLoS ONE 14(8): e0220311. <https://doi.org/10.1371/journal.pone.0220311>

**Editor:** Antimo Migliaccio, Universita degli Studi della Campania Luigi Vanvitelli, ITALY

**Received:** December 21, 2018

**Accepted:** July 12, 2019

**Published:** August 13, 2019

**Copyright:** © 2019 Palaniappan et al. This is an open access article distributed under the terms of the [Creative Commons Attribution License](https://creativecommons.org/licenses/by/4.0/), which permits unrestricted use, distribution, and reproduction in any medium, provided the original author and source are credited.

**Data Availability Statement:** The minimal dataset underlying the results in this study are available in the manuscript and as supplemental materials. RNA-seq and ER $\alpha$  ChIP-seq data are deposited in the Gene Expression Omnibus (GEO, Accession number GSE130032).

**Funding:** This work was supported by funding from CPRIT grant RP110471-P3. The funders had no role in study design, data collection and analysis, decision to publish, or preparation of the manuscript.

## Abstract

Estrogen receptor  $\alpha$  (ER $\alpha$ ) is the major driving transcription factor in the mammary gland development as well as breast cancer initiation and progression. However, the genomic landscape of ER $\alpha$  binding sites in the normal mouse mammary gland has not been completely elucidated. Here, we mapped genome-wide ER $\alpha$  binding events by chromatin immunoprecipitation followed by high-throughput sequencing (ChIP-seq) in the mouse mammary gland in response to estradiol. We identified 6237 high confidence ER $\alpha$  binding sites in two biological replicates and showed that many of these were located at distal enhancer regions. Furthermore, we discovered 3686 unique genes in the mouse genome that recruit ER in response to estradiol. Interrogation of ER-DNA binding sites in ER-positive luminal epithelial cells showed that the ERE, PAX2, SF1, and AP1 motifs were highly enriched at distal enhancer regions. In addition, comprehensive transcriptome analysis by RNA-seq revealed that 493 genes are differentially regulated by acute treatment with estradiol in the mouse mammary gland *in vivo*. Through integration of RNA-seq and ER $\alpha$  ChIP-seq data, we uncovered a novel ER $\alpha$  targetome in mouse mammary epithelial cells. Taken together, our study has identified the genomic landscape of ER $\alpha$  binding events in mouse mammary epithelial cells. Furthermore, our study also highlights the cis-regulatory elements and cofactors that are involved in estrogen signaling and may contribute to ductal elongation in the normal mouse mammary gland.

## Introduction

Estrogen is a key hormone for mammary epithelial proliferation during the mammary gland development, as well as during breast cancer initiation and progression [1–4]. The genomic

**Competing interests:** The authors have declared that no competing interests exist.

action of estrogen is mediated through two members of the nuclear receptor family, estrogen receptor  $\alpha$  (ER $\alpha$ ) and ER $\beta$  [5]. Of these two receptors, ER $\alpha$  plays a dominant role in mammary gland development, function, and tumorigenesis [6–9]. The classical pathway of estrogen action involves estrogen binding to the estrogen receptor, resulting in receptor dimerization and ligand-receptor complex entering into the nucleus where it then binds directly to the genomic DNA containing estrogen response elements (EREs) of the target genes. Various coregulators are then recruited to the gene promoter and/or distal enhancer region to modulate ER-mediated gene transcription [10, 11]. In the non-classical pathway, ligand-receptor complexes bind indirectly to genomic regions by tethering to other transcription factors, including the activator protein 1 (AP-1) families of transcription factors (TFs), members of the specificity protein 1 (SP1), and nuclear factor kappa-light-chain-enhancer of activated B cells (NF- $\kappa$ B), which lead to recruitment of chromatin-modifying coregulator proteins and allow activation or repression of ER target genes to drive cell proliferation [12–14].

In the mammary gland, ER $\alpha$  is the major receptor operating during ductal morphogenesis, as determined by the analysis of knockout phenotypes in mice [15]. Studies have shown that deletion of ER $\alpha$  inhibits development of the rudimentary ductal structure, and signaling from estradiol through ER $\alpha$  during puberty is required for mammary epithelial proliferation, ductal elongation, bifurcation, and invasion throughout the mammary fat pad [8, 16, 17]. Further, it has been shown that only a subset of luminal epithelial cells express ER $\alpha$  and estrogen promotes mammary epithelial cell proliferation by inducing amphiregulin (*Areg*), an epidermal growth factor (EGF) receptor ligand produced in ER $\alpha$  positive cells. *Areg* acts through a paracrine mechanism on neighboring ER-negative mammary epithelial and stromal cells to mediate estrogen-induced cell proliferation that drives ductal elongation [18, 19]. The processes of normal postnatal mammary gland development display many of the properties associated with breast cancer progression such as proliferation, invasion, angiogenesis, and resistance to apoptosis [20].

Several studies have focused on studying genome-wide ER binding sites in ER-positive breast cancer cell lines [21–26]. This approach has helped to identify the cis-regulatory elements and cofactors that are involved in mediating ER binding and ER target gene transcription in breast cancer cells. These studies have shown that the vast majority of ER binding sites are located at distal enhancer regions [21–23]. Furthermore, Brown and colleagues discovered that ER binding regions were enriched for the FOXA1 binding motif. Subsequently, FOXA1 was then identified as a pioneer factor for ER-chromatin interactions in ER-positive breast cancer cells [27, 28]. Genome-wide mapping of FOXA1 binding demonstrated that more than 50% of FOXA1 binding sites overlapped with ER binding events in ER-positive breast cancer cells [29]. In addition to FOXA1, studies have implicated GATA3 and PBX1 as pioneer factors for ER-chromatin interactions, since depletion of these transcription factors leads to reduction of ER binding events and transcriptional activity in response to estrogen [30, 31]. Furthermore, it has been shown that GATA3 acts upstream of FOXA1 in the ER binding [31].

Recently, Carroll and colleagues also mapped ER binding events in primary breast cancer samples from patients with different clinical outcomes [32]. The authors found that a subset of ER binding sites is maintained in good outcome, poor outcome, and metastatic breast tumors. Differential binding analysis revealed that ER binding events can discriminate between good and poor outcome tumors. Furthermore, motif analysis revealed that ERE motif is only enriched in good outcome ER-bound genomic regions, indicating that FOXA1 is not involved in these ER binding regions. On the other hand, in poor outcome tumors, ER binding events were associated with ERE and FOXA1 motifs. Nonetheless, it should be noted that genome-wide ER binding studies have been limited to ER-positive breast cancer cell lines and primary breast cancer samples, not the normal mammary gland. Although one recent study has shown

ER binding sites in the developing mouse mammary gland, this study focused only on control mammary glands which have not received any hormonal treatment [33].

Given the potential involvement of ER $\alpha$  in mammary gland development, as well as in breast cancer initiation and progression, we investigated for the first time, genome-wide ER $\alpha$  binding events by chromatin immunoprecipitation followed by high-throughput sequencing in mouse mammary gland under *in vivo* conditions of acute treatment with estradiol. Furthermore, we also used genome-wide transcriptome profiling (RNA-seq) to uncover the global transcriptome response to estradiol. This combined system approaches allowed us to identify the ER targetome in the mammary gland and this ER targetome consists of a subset of ER-regulated target genes whose acute regulation by estradiol is associated with direct binding to ER in luminal epithelial cells. Overall, our study provides a unique resource for the mechanisms underlying estrogen regulated gene expression in the mouse mammary gland.

## Materials and methods

### Mice

Animal experiments were approved by the Institutional Animal Care and Use Committee (IACUC) at Baylor College of Medicine (Houston, TX). BALB/cJ mice were purchased from The Jackson Laboratory (Bar Harbor, ME). All mice were housed in the animal facility at Baylor College of Medicine and maintained in a conventional mouse facility with room temperature set at 22°C with food and water provided *ad libitum*. The animal facility is accredited by the American Association of Laboratory Animal Care.

**Hormone treatments.** At 6 weeks of age, mice were ovariectomized and rested for 10 days and then mice were injected subcutaneously with sesame oil (50 $\mu$ l) or 17 $\beta$ -estradiol (100ng) for 2 hours. Sesame oil and 17 $\beta$ -estradiol were purchased from Sigma. After 2 hours, mice were sacrificed and both inguinal mammary glands (#4 mammary glands) were harvested from each mouse. The lymph node was removed from the # 4 mammary glands and used for RNA-seq and ChIP-seq analysis.

**Total RNA isolation.** For RNA-seq and quantitative Real-Time PCR (qPCR), total mammary gland RNA was isolated from #4 glands using the RNeasy Lipid Tissue Midi Kit according to the manufacturer's instructions (QIAGEN, Inc., Valencia, CA). To avoid potential contamination from muscle, only inguinal (rather than thoracic) glands were used in this study. Physical integrity of the RNA was assessed using the Agilent 2100 Bioanalyzer (Agilent Technologies, Inc., Santa Clara, CA). RNA quantitation was performed using the Nanodrop ND1000 spectrophotometer (Nanodrop Technologies, Wilmington, DE). For qPCR and RNA-seq analysis, total RNA pooled from a set of four to five mice per treatment group was analyzed. To ensure statistical significance, three separate sets of mice (12–15 mice in total) per treatment group were used in qPCR experiment.

**RNA-seq library preparation and sequencing.** Total RNA samples with RNA integrity number (RIN)  $\geq 8$  were used for transcriptome sequencing. Total RNA (10ng) was used for amplified double-stranded cDNA using the Ovation RNA-Seq System (NuGEN, San Carlos, CA). Double-stranded DNA was sheared to 200-300bp using the Covaris S2 sonicator (Covaris, Woburn, MA) and ligated to Illumina paired-end adaptors using the Illumina TruSeq DNA library preparation kit according to the manufacturer's instructions (Illumina, San Diego, CA). PCR amplification was performed to obtain the final cDNA library. Bioanalyzer 2100 (Agilent Technologies, Santa Clara, CA) analysis was used to verify fragment size after amplification, library size and concentration before clustering. A total of 10pM of the library was then used for paired-end sequencing on the HiSeq 2500 at the Genomic and RNA Profiling Core in Baylor College of Medicine.

**Quantitative Real-Time PCR.** RNA-seq was validated by qPCR. First, RNA was reverse transcribed using the High Capacity cDNA Reverse Transcription Kit (Applied Biosystems, Foster City, CA). TaqMan Universal PCR chemistry was implemented and tested on the ABI Prism PE7700 Sequence Detection System according to the manufacturer's instructions (Applied Biosystems). Standard curves were generated using a serial dilution of Mouse Universal Reference Total RNA (Clontech, Mountain View, CA). All experiments were performed in triplicate using three independent cDNA sets per treatment and normalized to cyclophilin D (*Ppid*). TaqMan Primer probes were purchased from Applied Biosystems (Foster City, CA) and are as follows: *Greb1* (Mm00479269\_m1), *Pgr* (Mm00435628\_m1), *Fos* (Mm00487425\_m1), *Areg* (Mm00437583\_m1), *Ccnd1* (Mm00432359\_m1), *Gata3* (Mm00484683\_m1), *Foxa1* (Mm00484713\_m1), *Cdh1* (Mm01247357\_m1), *Krt8* (Mm04209403\_g1), *Krt18* (Mm01601704\_g1), *Krt7* (Mm00466676\_m1), *Muc1* (Mm00449604\_m1), *Krt4* (Mm01296260\_m), *Csf1* (Mm00432686\_m1), *Bmp8a* (Mm00432109\_m), *Heyl* (Mm00516558\_m1), *Errfi1* (Mm00505292\_m1), *Six1* (Mm00808212\_m1), *Gata6* (Mm00802636\_m1), and *Ppid* (Mm00835365\_g1).

**ChIP-seq analysis.** For chromatin immunoprecipitation coupled with parallel sequencing (ChIP-seq) analysis, #4 mammary glands were pooled from six mice per replicate and two biological replicates were used for ER $\alpha$  ChIP-seq. Mammary glands were cut into small pieces and fixed in 1% formaldehyde for 15 min and quenched with 0.125M glycine for 5 min at room temperature. Mammary gland chromatin was prepared using ChIP-IT High Sensitivity Kit (Active Motif, Carlsbad, CA) according to the manufacturer's instructions. Briefly, the tissue pieces were homogenized using hand-held tissue homogenizer for 30 seconds and then spun down and washed twice with PBS. Chromatin was isolated from cell pellets by adding 5 ml of chromatin preparation buffer supplemented with Protease Inhibitor Cocktail and phenylmethanesulfonylfluoride (PMSF), followed by disruption of resuspended cell pellets with a Dounce homogenizer. Samples were pelleted by centrifugation and resuspended with ChIP buffer supplemented with protease inhibitor cocktail and PMSF. Lysates were sonicated and DNA was sheared to an average length of 150-500bp. Input DNA was prepared by treating aliquots with RNase, proteinase K, and heat to reverse crosslinks. The DNA was then purified by QIAquick PCR Purification Kit (QIAGEN, Inc., Valencia, CA) according to the manufacturer's instructions. Sonication efficiency was verified by agarose gel electrophoresis.

An aliquot of chromatin (~ 60ug) was precleared with protein G agarose beads (Active Motif, Carlsbad, CA). ChIP reactions were performed using an antibody against ER $\alpha$  (sc-542, Santa Cruz Biotechnology, Santa Cruz, CA). After incubation at 4°C overnight, protein G agarose beads were used to isolate the immune complexes and were washed, eluted from beads with elution buffer, and then subjected to RNase and proteinase K treatment. Crosslinks were reversed by incubation overnight at 65°C and ChIP DNA was purified by DNA purification kit (Active Motif, Carlsbad, CA). ER $\alpha$  ChIP enrichment was verified by qPCR using positive (*Greb1*) and negative (*Untr6*) targets. The resulting signals were normalized to input DNA.

**ChIP-seq library preparation and sequencing.** ChIP DNA library construction was performed by using ThruPlex DNA-seq Kit (Rubicon Genomics, Ann Arbor, MI) according to the manufacturer's instructions. Briefly, 10  $\mu$ l of ChIP DNA or 10 ng of input DNA was used for library construction and PCR amplification was performed to obtain the final library. AMPure XP beads were used for library purification and purified libraries were analyzed in Bioanalyzer 2100 (Agilent Technologies, Santa Clara, CA) to verify fragment size after amplification, library size and concentration before clustering. A total of 10pM of the library was then used for single-end sequencing on the HiSeq 2500 at the Genomic and RNA Profiling Core in Baylor College of Medicine. Sequences (51-nt reads) were aligned to the mouse genome (mm9) using the BWA algorithm. Aligns were extended in silico at their 3'-ends to a length of 150bp and assigned to 32-nt bins along the genome. The resulting histograms were stored as

Binary Analysis Results (BAR) files. Peak locations were determined using the Model-based Analysis of ChIP-seq Algorithm (MACS) with a  $p$ -value cutoff of  $1E-8$ .

**Validation of ER $\alpha$  -binding sites by ChIP-quantitative PCR.** ER $\alpha$  ChIP was performed as described above in the ChIP-seq analysis. ChIP DNA and input DNA were analyzed by qPCR using SYBR Green Master Mix. Primers were generated corresponding to the regions identified by our ChIP-seq. The enrichment of ER $\alpha$ -binding found in each sample was normalized to input values. For primer sequences, see [S1 Table](#).

## Bioinformatics

The web-based application Galaxy (<http://galaxyproject.org>) was used to intersect the binding regions from the ChIP-seq replicates [34–36]. Cross-correlation analysis was performed using phantompeakqualtools (<https://www.encodeproject.org/software/phantompeakqualtools/>) [37]. Cistrome (<http://cistrome.org/ap/>) was used to construct the correlation plot, conservation plot, and SeqPos Motif discovery analyses [38]. HOMER (Hypergeometric Optimization of Motif EnRichment) was used for Motif Discovery [39]. Integrative Genomics Viewer (IGV) was used to generate custom annotation tracks to view ER $\alpha$  binding in relation to specific genes (<http://www.broadinstitute.org/igv>). Enriched gene ontology (GO) terms were identified using the DAVID Functional Annotation Tool (<http://david.abcc.ncifcrf.gov/summary.jsp>) [40]. Principle component analysis and Euclidean distances-based clustering were performed using the normalized and log-transformed read counts.

**Accession numbers.** RNA-seq and ER $\alpha$  ChIP-seq data were deposited in the Gene Expression Omnibus (GEO, Accession number GSE130032).

**Statistical analysis.** Data are presented as mean $\pm$ SEM. The significance of the differences between groups was determined by Student's  $t$ -test. Values were considered statistically significant at  $p < 0.05$ .

## Results

### Genome-wide analysis of ER $\alpha$ binding sites

We mapped ER $\alpha$  binding events using chromatin immunoprecipitation followed by deep sequencing on mammary glands collected from ovariectomized mice that had been treated with estradiol for 2 hours. To ensure a robust and precise representation of the ER $\alpha$  binding sites in the mammary gland, we employed two independent biological replicates for ER $\alpha$  ChIP-seq analysis. Binding events were called using the MACS model based peak finding algorithm. A  $p$ -value cutoff  $1E-8$  identified 9607 binding regions in replicate 1 and 6819 binding regions in replicate 2. The total number of reads and uniquely mapped reads for each sample is shown in [S2 Table](#). By using the web-based application Galaxy/Cistrome, intersection of the two biological replicates showed 78% of binding site concordance. This analysis yielded 6237 common ER binding events in mammary epithelial cells mapped near 3686 unique genes after acute treatment with estradiol ([Fig 1A](#)). A heatmap was generated for visualization of the 6237 common ER $\alpha$  peaks found in both replicates ([Fig 1B](#)). We used Pearson's correlation method to compare two biological replicates. As shown in [Fig 1C](#), Pearson's correlation was very high ( $r = 0.95$ ) between the two biological replicates suggesting that good reproducibility between the two replicate samples. Comparison of the sequences from ER intervals within various placental mammalian genomes showed a strong level of conservation in the regions of ER $\alpha$  binding only and not in surrounding regions ([Fig 1D](#)). Furthermore, we also performed cross-correlation analysis in ER $\alpha$  ChIP replicate 1 and 2. We observed two cross-correlation peaks one corresponding to the read length (Phantom peak) and other one to the average fragment length of library suggesting that our ChIP-seq is robust ([S1 Fig](#)).



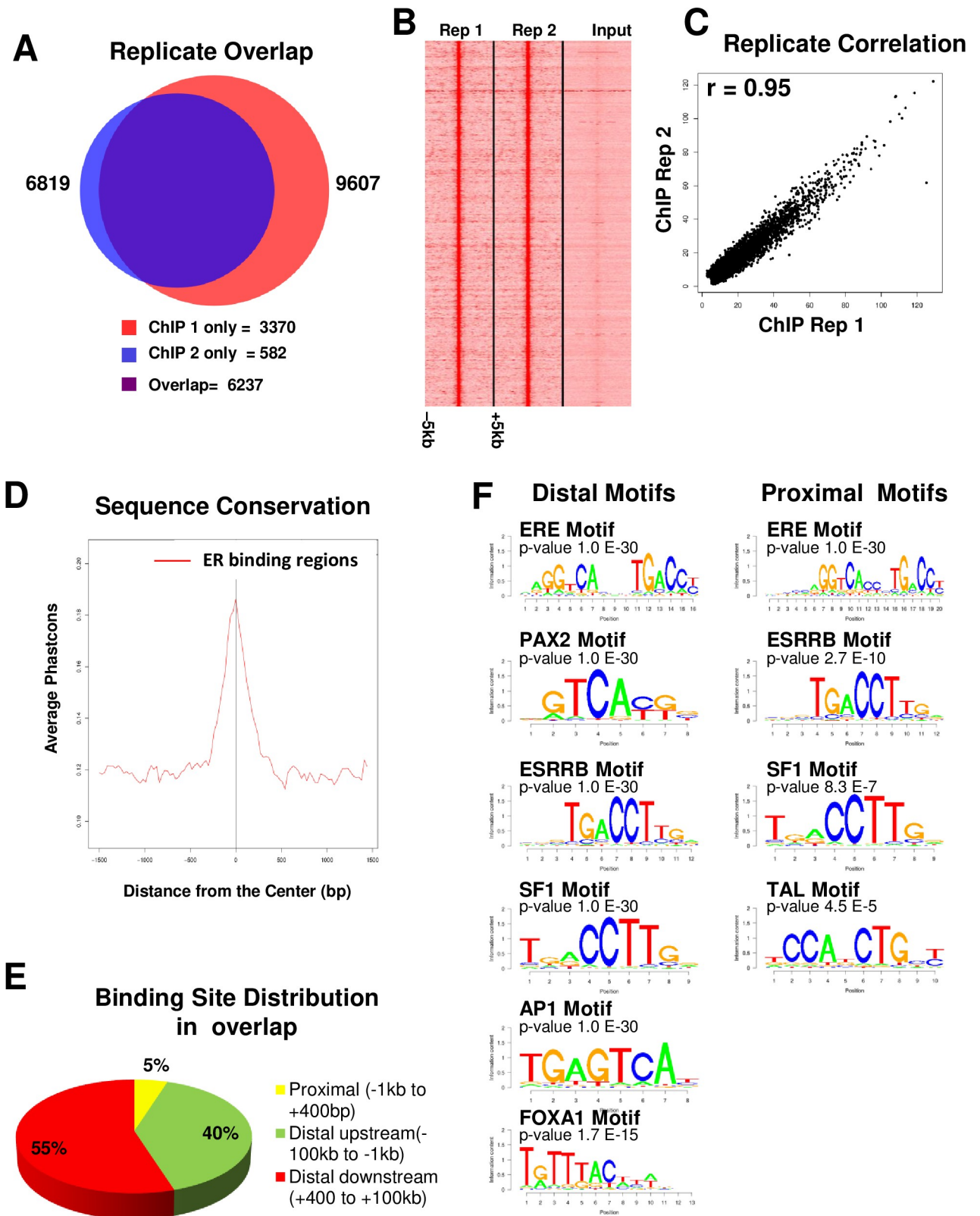


**Fig 1. Validation of ER $\alpha$  ChIP-seq accuracy, binding sites distribution and motif enrichment.** (A) Proportional Venn diagram representing the intersection of ER $\alpha$  binding sites identified in two ChIP-seq replicates; Six mice per replicate. (B) Heatmap showing ER $\alpha$  binding events found in the mammary gland after 2h of treatment with estradiol (ER $\alpha$  ChIP-seq replicate 1 and 2 [left] and input [right]). The window shows  $\pm$ 5kb regions from the

center of the binding sites. (C) Pearson correlation of the ER $\alpha$  binding sites of two ChIP-seq replicates ( $r = 0.95$ ). (D) Conservation plot of mouse ER $\alpha$  binding sites with high conservation around peak centers compared to flanking regions. (E) Distribution of ER $\alpha$  binding sites in the overlap of ER $\alpha$  binding events were identified in two ChIP-seq replicates. (F) SeqPos motif enrichment in distal (up and down) and proximal regions of ER $\alpha$  binding sites.

<https://doi.org/10.1371/journal.pone.0220311.g001>

We next analyzed ER $\alpha$  binding site distribution in this data set. ER $\alpha$  binding sites were divided into three categories; distal upstream (-100kb to -1kb), proximal (-1kb to +400 bp), and distal downstream (+400 bp to +100kb), based on the peak locations relative to RefSeq genes. In this analysis, binding sites were assigned to the nearest transcription start site (TSS). As shown in Fig 1E, only 5% of ER $\alpha$  binding sites were distributed in the proximal region. However, majority of ER $\alpha$  binding sites were located in the distal upstream (40%) and downstream (55%) regions. These results indicate that the vast majority of ER $\alpha$  binding sites are located at the distal regions of ER target genes in the mouse mammary gland which is consistent with ER binding sites in ER-positive breast cancer cells [21–23]. Further, it has been shown that distal ER $\alpha$  binding sites are anchored at gene promoters through long-range chromatin interactions, suggesting that ER $\alpha$  functions by bringing genes together for coordinated transcriptional regulation by chromatin looping [41]

### Motif analysis

To discover the network of transcription factors linked with genomic binding of ER $\alpha$ , we employed the Cistrome tool SeqPos and identified enriched binding motifs within the proximal and distal regulatory regions of ER $\alpha$  binding sites. In the distal regions (up and down) of ER $\alpha$  binding sites contained a canonical ERE and other motifs including PAX2, ESRRB, SF1, and AP1 motifs as the most highly enriched ( $p$ -value  $< 10^{-30}$ ) cis-elements. Additionally, there was substantial enrichment of FOXA1 motif in the distal ER $\alpha$  binding regions which is consistent with previously reported data that FOXA1 acts as an important pioneer factor for ER chromatin interaction in luminal breast cancer cells [27–29]. The proximal region (-1kb to +400bp) of ER $\alpha$  binding sites contained canonical ERE as the most significantly enriched motif, along with other significantly enriched motifs such as ESRRB, SF1 and TAL (Fig 1F). The complete motifs enrichment is included in S3 Table. Furthermore, we also performed motif enrichment analysis by using HOMER in the overlapped ER binding sites (regardless of binding site distribution). As expected, most of the motifs identified by Cistrome were confirmed by HOMER. The complete HOMER motifs enrichment is also included in S4 Table.

### Validation of ER $\alpha$ binding by ChIP qPCR

We next interrogated several known estrogen-regulated genes for their ability to recruit ER $\alpha$  in an estrogen-dependent manner. To test this, mammary gland chromatin was isolated from ovariectomized mice that had been treated with vehicle or estradiol for 2 hours and then subjected to ER $\alpha$  ChIP followed by qPCR as described in the Materials and Methods. Our ChIP-seq data have identified several ER $\alpha$  binding sites in the distal upstream region of the *Greb1* gene (Fig 2A). Of these, we verified two of the ER $\alpha$  binding sites (-3281 and -33380) by ChIP qPCR. As shown in Fig 2A, ER $\alpha$  was highly enriched in these regions in response to estradiol treatment, confirming direct estradiol-dependent ER $\alpha$  recruitment to *Greb1*. Our ER $\alpha$  ChIP-seq analysis revealed peak of ER $\alpha$  binding of progesterone receptor (*Pgr*) in the distal downstream region (+70663) which was independently verified by ChIP qPCR (Fig 2B). Furthermore, our ChIP-seq data also discovered ER $\alpha$  binding in the distal downstream regions of *Fos*, *Gata3*, and *Areg* genes (Fig 2C–2E) and these binding sites were validated by ChIP qPCR in an estradiol-dependent manner (Fig 2C–2E). Collectively, our ER $\alpha$  ChIP-seq was independently confirmed by ChIP qPCR.

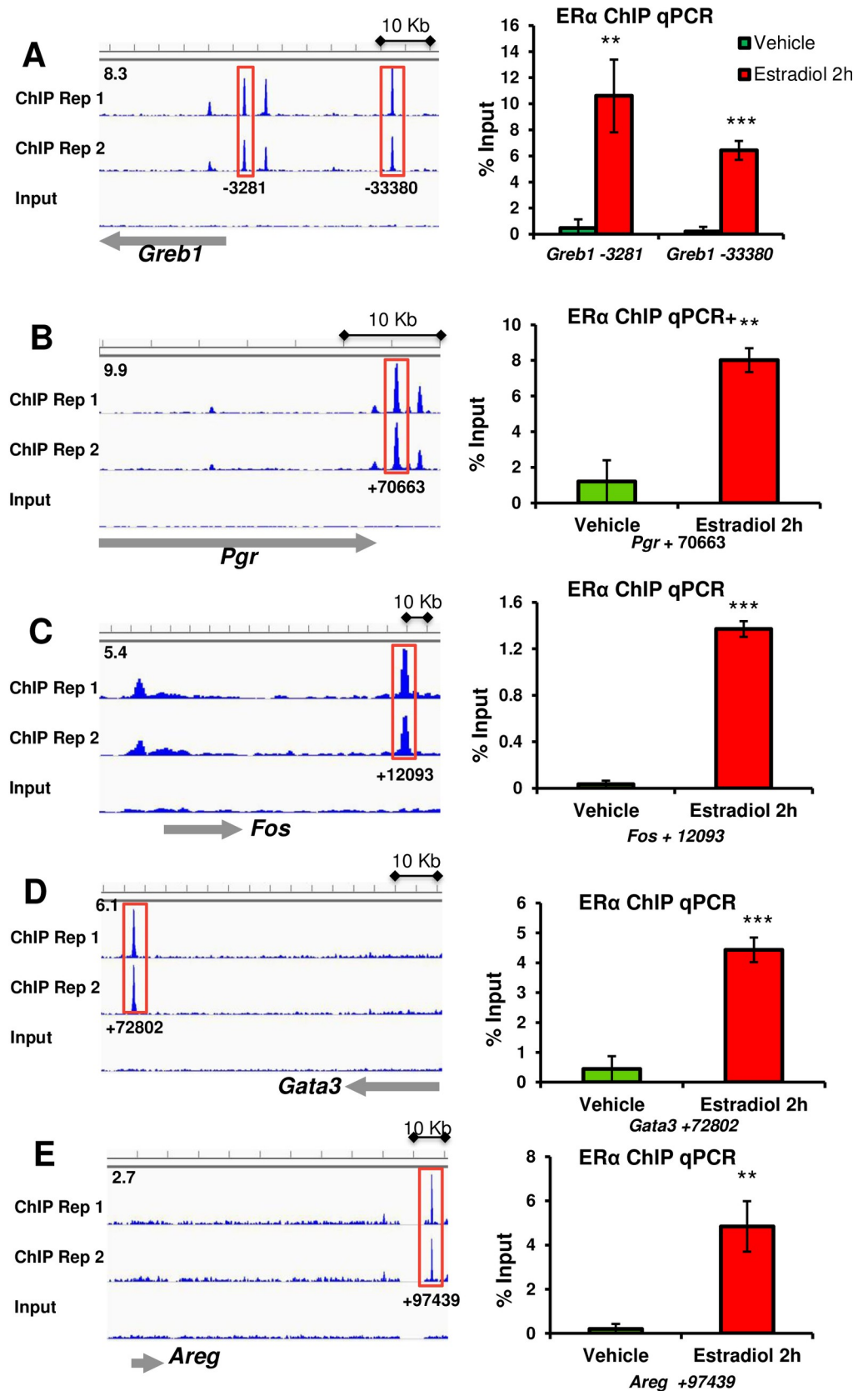




**Fig 2. Representative screen shots of ChIP-seq data showing gene ER $\alpha$  recruitment at 2 hours after exposure to estradiol** IGV screen shots showing ER $\alpha$  binding sites in relation to the TSS of (A) *Greb1*, (B) *Pgr*, (C) *Fos* (D) *Gata3* and (E) *Areg*. Peak locations relative to the TSS are listed below each screen shot and the numbers indicate peak value of each gene. Red boxes represent peaks that were validated by ChIP-qPCR. Graphs representing validation of ER $\alpha$  occupancy using ChIP followed by qPCR for *Greb1*, *Pgr*, *Fos*, *Gata3* and *Areg*. A total of six mice per replicate; Results are means  $\pm$  SEM of three independent experimental replicates. \*\*,  $p < 0.01$ ; \*\*\*,  $p < 0.001$ .

<https://doi.org/10.1371/journal.pone.0220311.g002>

## Genome-wide transcriptome analysis of ER-target genes

To disclose the global gene signatures that are acutely regulated by estradiol, we next performed genome-wide transcriptome analysis in the mammary gland of ovariectomized mice treated with vehicle or estradiol for 2 hours. We used biological replicate pools of mammary glands from 5 mice per pool for total RNA isolation and then subjected to global gene expression analysis by RNA-seq as described in the Material and Methods. The reads were mapped to the mouse Ensembl reference set of 82,508 transcripts (annotated to 31034 genes) using TopHat. Relative transcript abundance was identified using the RSEM algorithm [42]. The edgeR package was used to identify differentially regulated gene expression [43]. The total number of reads and uniquely mapped reads for each sample is shown in S2 Table. Data quality was assessed using principal component analysis (PCA) and clustering of RNA-seq samples using Euclidean distance. Our PCA plot of the four RNA-seq samples showed that the control and estradiol samples are well separated along the principal component 1 (PC1) which explained the 75% of the total variance (S2A Fig). Further, we also used the Euclidean sample distances to show that the samples from the same conditions are well clustered (S2B Fig). We identified 493 genes differentially regulated due to an acute treatment with estradiol. We observed that 220 genes (45%) were upregulated and 273 (55%) genes were downregulated at  $FDR < 0.05$  (S5 Table). A heatmap was also generated to show the differentially regulated genes (Fig 3A). We used Pearson's correlation method to compare two biological replicates. As shown in Fig 3B, Pearson's correlation was very high ( $r = 0.96$ ) between the two biological replicates for both the vehicle and estradiol treated groups suggesting that our RNA-seq is robust. Next, we applied a bioinformatics approach, Ingenuity Pathways Analysis (IPA) (Ingenuity, CA), to identify a potential network based on the regulated genes to unveil the molecular mechanisms of estradiol action in the mammary gland. Using this approach, we identified  $\beta$ -estradiol ( $p = 9.46E-21$ ) and TGF $\beta$  ( $p = 5.75E-19$ ) as the top upstream regulators (data not shown). As expected, these signaling cascades were predicted to be activated by acute treatment with estradiol treatment. The most enriched gene networks were centered on FOS, a classical estrogen target gene (Fig 3C). Studies have shown that FOS has been implicated to regulate cell proliferation, differentiation, and transformation [44, 45]. Furthermore, DAVID functional annotation analysis was also used to identify the biological function of differentially regulated genes. Gene signatures-induced by estradiol were enriched for GO terms associated with negative regulation of protein kinase activity, epithelium development, regulation of cell proliferation and morphogenesis of a branching structure. However, genes repressed by estradiol were enriched for GO terms associated with muscle contraction, mammary gland development, epithelial cell differentiation, gland morphogenesis and epithelium development (Fig 3D). The complete GO terms analysis is included in S6 Table.

## Validation of RNA-seq by qPCR

To validate our RNA-seq data, we measured the expression of well-established estradiol responsive genes by qPCR. To examine this, 6-week old female mice were ovariectomized and then rested for 10 days. After 10 days, mice were treated with vehicle or estradiol for 2 hours

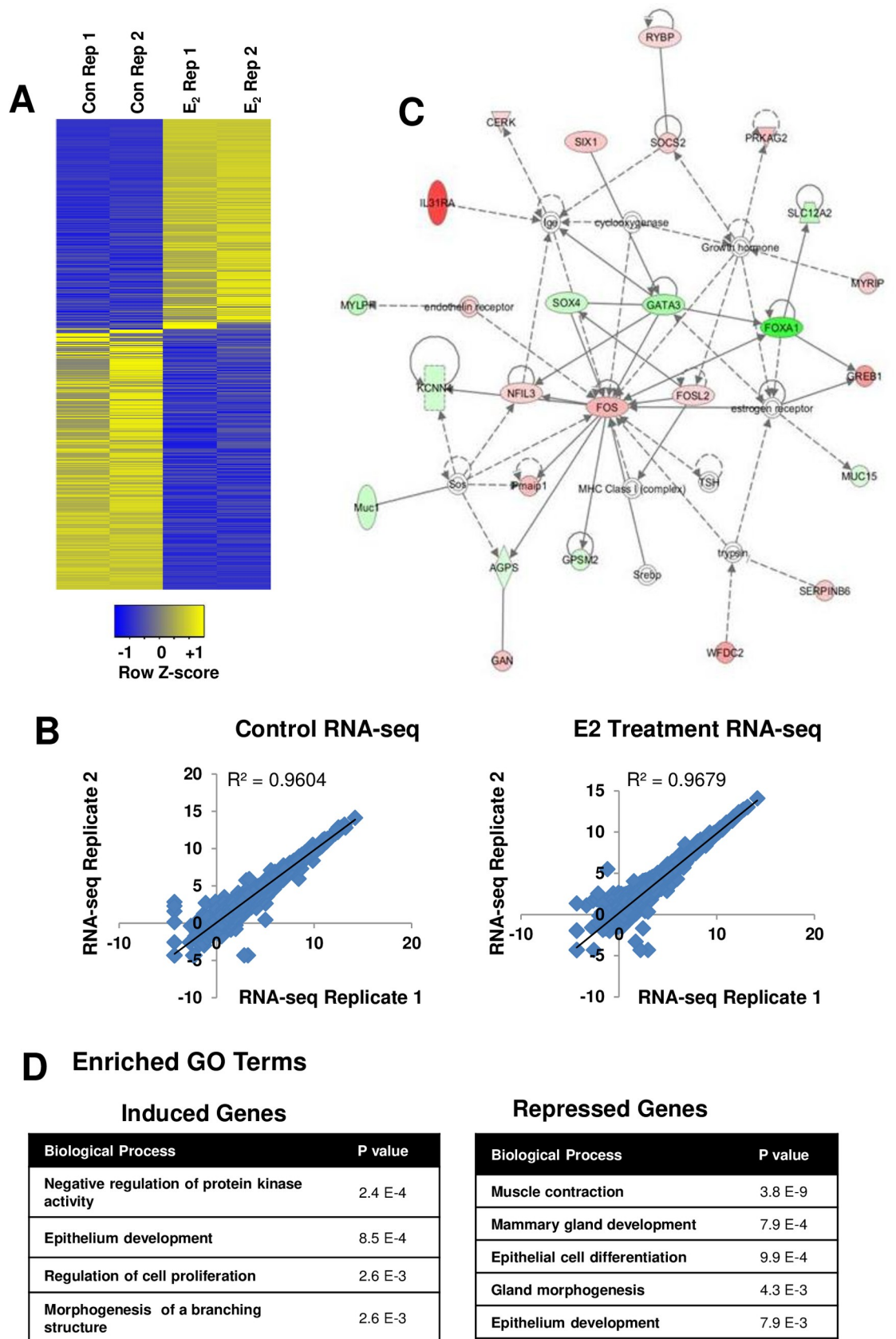


**Fig 3. Global gene expression analysis in mouse mammary gland.** (A) Heatmap of 493 genes (FDR<0.05) that are differentially expressed between mammary gland samples from vehicle (2 h) and estradiol (2 h) treatment. Duplicate pools of mammary glands from mice (5 mice per pool) were used for RNA-seq analyses under each treatment condition. (B) Pearson correlation of RNA-seq replicates (Control  $r = 0.96$  and estrogen treatment = 0.96). (C) Ingenuity Pathway Analysis of RNA-seq. Interactions of estrogen regulated genes was analyzed by Ingenuity Pathway Analysis. A top enriched molecular network revolves around FOS. Red color indicates upregulated genes and green color indicates downregulated genes after acute treatment with estradiol. (D) Summary of enriched GO terms (FDR< 0.05) of ER target genes induced and repressed at 2 h after estradiol treatment using the DAVID Functional Annotation Tool.

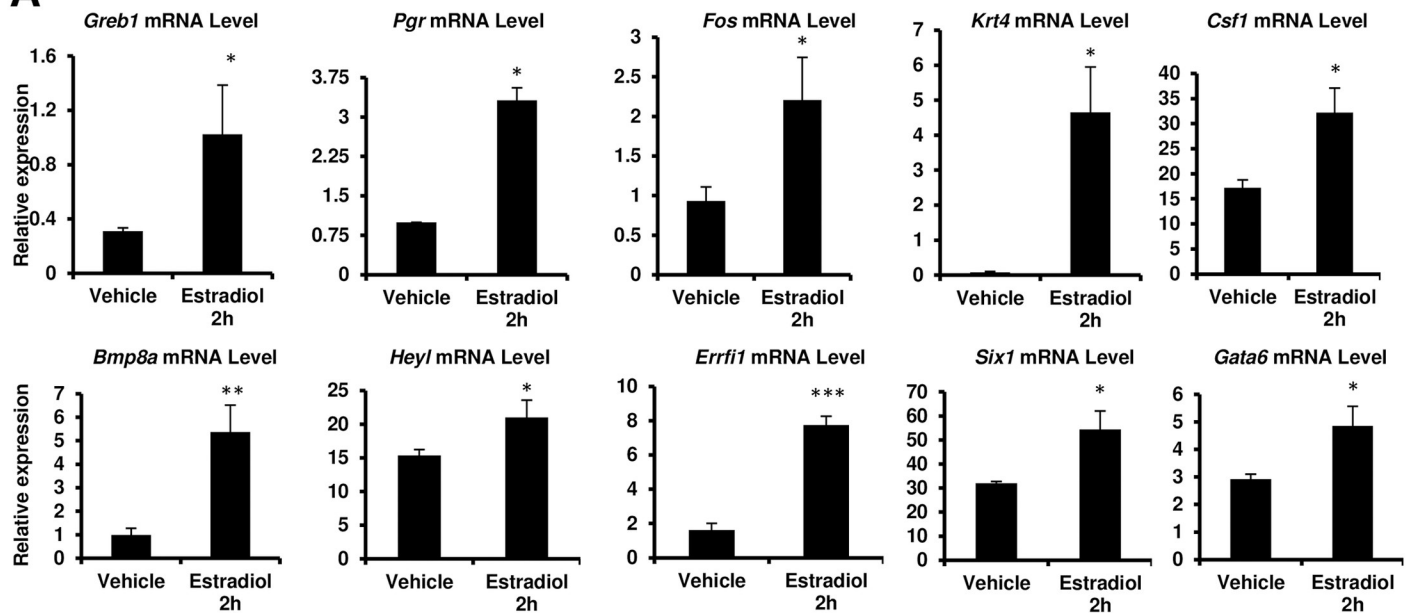
<https://doi.org/10.1371/journal.pone.0220311.g003>

and #4 mammary glands were harvested. We used triplicate pools of mammary glands from vehicle or estradiol treated mice (4–5 mice per pool) for RNA isolation and subjected to qPCR. First, we tested estradiol-induced genes. Studies have shown that *Greb1*, *Pgr*, and *Fos* are canonical ER target genes [27–29]. Our RNA-seq analysis revealed that these genes were induced more than 2-fold by acute treatment with estradiol. Similar to what we observed in the RNA-seq data, acute estradiol treatment caused a significant increase in mRNA levels of *Greb1*, *Pgr*, and *Fos* expression in the mammary gland (Fig 4A). Our ChIP-seq analysis also identified ER $\alpha$  binding sites near these genes and confirmed direct hormone-dependent ER recruitment to these genes (Fig 2A–2C). Interestingly, our RNA-seq also identified several known genes (*Krt4* and *Csf1*) as well as previously unidentified estrogen target genes such as *Bmp8a*, *Heyl*, *Errfi1*, *Six1*, and *Gata6*. These estrogen-induced genes were independently confirmed by qPCR (Fig 4A). Our RNA-seq analysis also revealed that acute *in vivo* treatment with estradiol significantly downregulated *Gata3*, *Foxa1*, *Areg*, and *Ccnd1* expression. These downregulated genes were independently confirmed by qPCR. As shown in Fig 4B, acute estradiol treatment caused more than a 2-fold reduction of *Gata3*, *Foxa1*, *Areg*, and *Ccnd1* mRNA levels when compared with vehicle treatment. The possible explanation for this observation is that a secondary transcriptional response may be involved in induction of these genes in response to estradiol signaling. Our acute treatment (2 hours) makes it unlikely that we will detect secondary changes in transcription. Further, it has been shown that estradiol treatment (24h) did not increase the *Ccnd1* and *Areg* mRNA levels. However, in the presence of progesterone treatment, these genes were dramatically increased suggesting that progesterone may also be required for these gene expression in the normal mouse mammary gland [46]. Indeed, Nuclear Receptor Signaling Atlas (NURSA) transcriptome database revealed that *Foxa1* and *Gata3* are downregulated in response to estradiol. Studies have shown that GATA3 is necessary for luminal epithelial cell differentiation and the gene is often mutated in human breast cancer [47–54]. Several direct downstream targets of GATA3 in the luminal epithelium have been identified including FOXA1, an important regulator of ER $\alpha$  expression. Notably, our ER $\alpha$  ChIP-seq identified a peak near the *Gata3* gene and confirmed direct estrogen-dependent ER $\alpha$  recruitment to *Gata3*. In addition, we also observed significant downregulation of several luminal cell makers such as *Cdh1*, *Muc1*, *Krt7*, *Krt8* and *KRT18* gene sets in acute treatment with estradiol treatment suggesting that maturation of luminal cells may be reduced (Fig 4B). Collectively, our data suggests that acute treatment with estradiol represses luminal cell differentiation leading to expansion of a de-differentiated epithelial cell population.

### Identification of ER $\alpha$ targetome in mammary epithelial cells

To identify subsets of estrogen-regulated genes that are direct targets of ER positive luminal epithelial cells, we integrated ER $\alpha$  ChIP-seq and RNA-seq data to uncover the subset of estrogen regulated genes that directly recruit ER $\alpha$  in ER positive luminal epithelial cells. In this analysis, we used the 220 estradiol-induced and 273 repressed genes identified after acute treatment with estradiol (Fig 3) to interrogate the 3686 unique ER binding genes. This integration

**A Induced genes**



**B Repressed genes**

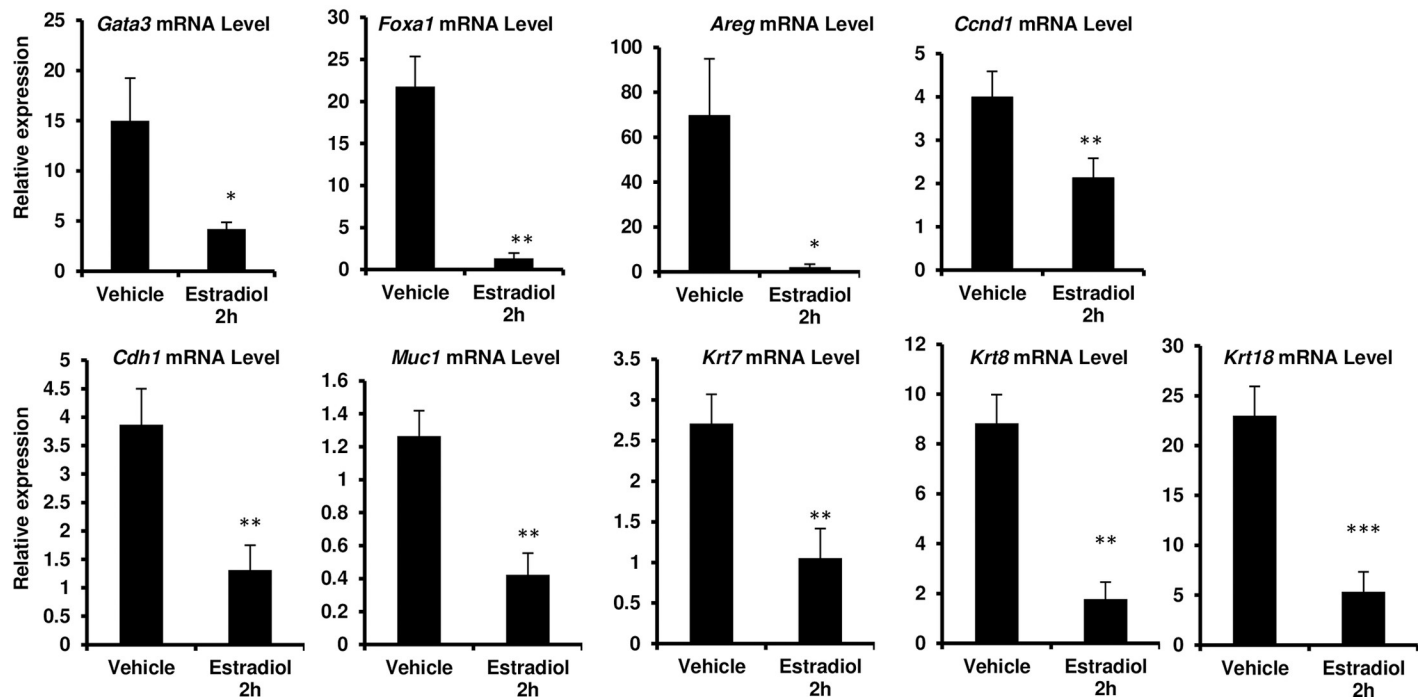


**Fig 4. Validation of estrogen regulated genes by qPCR.** Quantitative Real-Time PCR validation of estradiol-induced (A) and repressed (B) genes. Expression of selected genes was normalized using *Ppid* as the internal control. A total of 4–5 mice per treatment replicate, tested in triplicate per treatment group. Results are means  $\pm$  SEM of three independent experimental replicates. \*,  $p < 0.05$ ; \*\*,  $p < 0.01$ ; \*\*\*,  $p < 0.001$ .

<https://doi.org/10.1371/journal.pone.0220311.g004>

showed that 36% (177 genes) of the 493 differentially regulated genes (220 induced and 273 repressed genes) directly recruit ER $\alpha$  (Fig 5A and 5D). These genes (177) are shown in S7 Table. Since ER $\alpha$  is expressed only in a subset of luminal epithelial cells, these genes could potentially represent a global estradiol-regulated luminal epithelial cell targetome of ER $\alpha$ .

We next analyzed ER $\alpha$  binding site distribution in the ER $\alpha$  targetome in mammary epithelial cells. Interrogation of the ER $\alpha$  binding site distribution in upregulated genes showed that only 7% ER $\alpha$  binding sites were distributed in the proximal region, defined as -1 kb to +400 bp. However, the vast majority of ER $\alpha$  binding sites were located in the distal upstream (defined as -1kb to -100kb) and downstream regions (defined as +400 bp to +100kb), 34% and 59%, respectively (Fig 5B). We performed the same analysis on genes repressed by estradiol treatment. As shown in Fig 5E, only 4% of genes are associated with ER $\alpha$  binding in the proximal region, 38% in the distal upstream, and 58% in the distal downstream. Taken together, our ER $\alpha$  targetome revealed that the majority of ER $\alpha$  binding is located in distal regions of genes in the mammary gland, which is consistent with previous reports of ER binding sites in ER-positive breast cancer cells [21–23].

To identify the network of transcription factors linked with the ER $\alpha$  targetome, we employed the Cistrome tool SeqPos and identified enriched binding motifs within the estradiol-induced and repressed genes associated with ER binding regions. ER target genes induced by estradiol contained a canonical ERE motif as the most highly enriched cis-element. Additionally, ESRRB, ATF2, de novo, PAX2, and PAX6 motifs were enriched in estradiol-induced genes (Fig 5C). However, ER $\alpha$  binding sites in genes repressed by estradiol showed a significant enrichment of ERE, ESRRB, and SF1 motifs (Fig 5F). The co-enrichment of PAX2 sites with ER $\alpha$  binding is consistent with a recognized role for PAX2 in human breast cancer cells [55]. PAX2 was shown to be expressed in a subset of breast cancers and was recruited to the ER binding site after both estrogen and tamoxifen treatment [55].

To identify the biological function of the ER $\alpha$  targetome, we again used DAVID functional annotation analysis. Interrogation of the 135 estrogen-induced ER $\alpha$  targetome identified a significant enrichment for GO terms associated with regulation of small GTPase mediated signal transduction, regulation of specific transcription from RNA polymerase II promoter, epithelial cell differentiation, growth and morphogenesis of a branching structure. On the other hand, analysis of the 42 genes comprising the estrogen-repressed ER targetome showed enrichment for GO terms associated with muscle contraction, response to inorganic substance, and response to inorganic substance (Fig 5G). The complete GO terms analysis is included in S8 Table.

## Discussion

In this study, we report for the first time a comprehensive analysis of ER $\alpha$  binding events which elucidates the molecular mechanism of ER $\alpha$  action in the normal mouse mammary gland *in vivo* in response to acute estradiol treatment. We have identified 6237 high-confidence ER $\alpha$  binding sites in two biological replicates. These binding regions also corresponded with 3686 unique genes in the mouse genome that recruit ER $\alpha$  in response to acute estradiol treatment. Recent studies have shown that ER interacts with DNA sites in the absence of ligand in breast cancer cells and mouse uterus [56, 57]. However, these ER chromatin binding sites are relatively lower than ligand-induced ER $\alpha$  binding sites. It has also been shown that ER binds the same chromatin binding sites regardless of the ligand; however, signal intensity was highest for estradiol treatment [29]. The distribution of ER $\alpha$  binding sites revealed that the majority of these sites (95%) are located in the distal enhancer, which is in agreement with other studies in ER-positive breast cancer cell lines [21, 22]. Our data also suggest that ER $\alpha$  interactions occur at distal sites under normal physiological conditions. Interrogation of ER $\alpha$ -DNA interaction sites revealed ERE, PAX2, SF1, and AP1 motifs were highly enriched at sites where ER $\alpha$  binds, suggesting that these transcription factors interact with DNA and contribute to stabilizing the ER complex on chromatin. Furthermore, our ER binding sites also identified



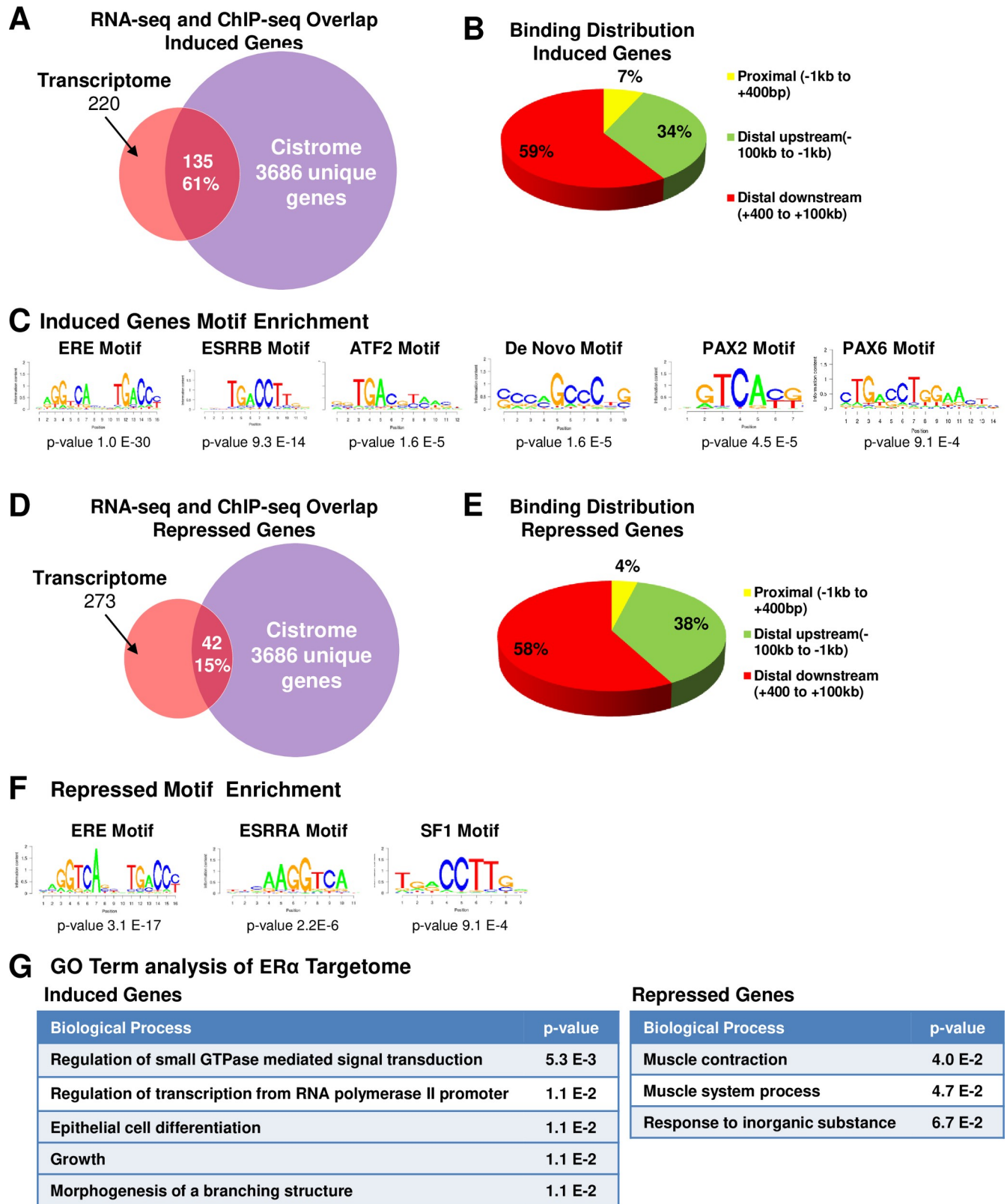


**Fig 5. ER $\alpha$  targetome in mammary epithelial cells.** (A) Proportional Venn diagram representing unique estradiol-induced genes at 2h has identified by RNA-seq (orange), unique genes with at least one ER $\alpha$  -binding region as detected by ChIP-seq (purple), and overlap indicates-induced genes at 2 h with at

least one ER binding site. (B) ER $\alpha$  binding distribution at genes induced by estradiol at 2 h. (C) SeqPos Motif enrichment in direct ER target genes was induced at 2 h after estradiol exposure. (D) Proportional Venn diagram representing unique estradiol-repressed genes at 2 h as detected by RNA-seq (orange), unique genes with at least one ER $\alpha$ -binding region as detected by ChIP-seq (purple), and estradiol-repressed genes at 2 h with at least one ER $\alpha$  binding site (overlap). (E) ER $\alpha$  binding distribution at genes was repressed by estradiol treatment. (F) SeqPos Motif enrichment in the direct ER target genes repressed at 2 h after estradiol exposure. (G) Enriched GO terms of ER targetome by using the DAVID functional annotation tool.

<https://doi.org/10.1371/journal.pone.0220311.g005>

the FOXA1 motif, whose expression is required for luminal epithelial ER $\alpha$  expression and post-pubertal development of the normal mammary gland [58]. FOXA1 is an established pioneer factor for the majority of ER $\alpha$  binding to the genome in human breast cancer cells [21, 29]. Whole transcriptome analysis by RNA-seq revealed that 493 genes are differentially regulated by acute treatment with estradiol in the mouse mammary gland *in vivo*. By integrating genome-wide ER $\alpha$  binding and global gene expression signatures, we uncovered a novel ER targetome of 177 genes that are associated with estrogen-dependent ductal elongation in the mouse mammary gland *in vivo*. This cistromic and transcriptome resource revealed the cis-regulatory elements and cofactors that are involved in estrogen signaling in the normal mouse mammary gland.

It is well documented that the ovarian hormones estrogen and progesterone act as master regulators of mammary gland development. Specifically, estrogen triggers ductal elongation during puberty whereas progesterone is involved in mammary gland side-branching [46, 59–61]. Studies have shown that estradiol-mediated activation of ER $\alpha$  signaling is required for ductal mammary epithelial cells to proliferate, leading to ductal outgrowth. Deletion of ER $\alpha$  results in normal mammary glands before puberty. However, after puberty, terminal end buds remained absent, and the failure of ducts to invade into the fat pad, suggesting that ER $\alpha$  action is essential for mammary gland development [16, 62]. Only subset of luminal epithelial cells are ER $\alpha$  positive, and release of paracrine signals from these ER-expressing cells permit other nearby epithelial cells, both luminal and myoepithelial, to participate directly in ductal outgrowth [16, 18].

In our whole genome transcriptome profiling using RNA-seq, we identified that ER-regulated genes were affected by acute treatment with estradiol in the mouse mammary gland *in vivo*. We discovered that 493 genes are differentially regulated by estradiol. According to DAVID functional annotation analysis, these differentially regulated genes are primarily involved in molecular and cellular processes ranging from epithelium development to morphogenesis of a branching structure. Furthermore, we validated the RNA-seq results independently by qPCR analysis to confirm that these genes were indeed regulated in the mammary gland in response to acute treatment with estradiol. For validation, we selected canonical ER target genes as well as previously unidentified ER target genes. Studies have shown that *Greb1*, *Pgr*, and *Fos* are classical estradiol target genes and are strongly induced by estradiol. ER $\alpha$  directly controls GREB1 expression, and GREB1 is required for breast cancer cell growth. Clinically, the loss or reduced expression of GREB1 is predictive of poor outcome and decreased relapse free survival, similar to ER status [63–67]. It is well documented that PR is an ER target gene and induces proliferation of neighboring cells primarily by a paracrine mechanism [68]. It has been shown that progesterone induces receptor activator for nuclear factor  $\kappa$ B ligand (RANKL) secretion from ER $\alpha$ + / PR+ mammary cells, and then this factor can directly binds to its receptor RANK to induce side-branching and alveolar development during ductal development and pregnancy [59, 69].

Fos is an immediate early gene acutely induced by intracellular signaling cascades [70]. Fos, along with other members of the Fos family, dimerize with Jun to form the AP-1 transcription factor complex which regulates many genes involved in proliferation, differentiation, and survival. In breast cancer cells the Fos gene also plays a key role in tumorigenesis and invasive

growth. Our data showed that estradiol induces expression of *Greb1*, *Pgr*, and *Fos* genes in the normal mouse mammary gland. Furthermore, our ER $\alpha$  ChIP-seq data confirmed that ER binds these genes at the distal region.

BMP8a is a member of transforming growth factor  $\beta$  (TGF $\beta$ ) and plays a central role in cell proliferation, differentiation, and survival [71]. A recent study showed that BMP8a acts as paracrine factor for estrogen-dependent regulation of epithelial cell proliferation in the uterus [72]. In the present study, we observed acute exposure to estradiol induced *Bmp8a* mRNA levels in the mammary gland, suggesting that *Bmp8a* may also act as a paracrine effector of estrogen-induced mammary epithelial cell proliferation. Furthermore, our ER $\alpha$  ChIP-seq data also identified ER $\alpha$  binding near *Bmp8a* gene, which was independently confirmed by ChIP qPCR (data not shown), suggesting that *Bmp8a* is also a direct target of ER $\alpha$  in the normal mammary gland.

GATA3 has been implicated in breast tumorigenesis and its highest expression was observed in the luminal subtype of breast cancer [73, 74]. Mutations in GATA3 have also been identified in a subset of breast cancers [75]. In the normal mouse mammary gland, *Gata3* is the most highly expressed transcription factor in the mammary epithelium [76]. Using a mammary epithelium-specific knockout of *Gata3*, it has been shown that *Gata3* is essential in maintaining luminal epithelial cell differentiation [48, 49]. Several direct downstream targets of GATA3 in the luminal epithelium have been identified including FOXA1, a key regulator of ER binding in the breast cancer cells. Furthermore, ER binds near the GATA3 gene in breast cancer cells, as shown through ChIP assays [21, 23, 77].

Our ER $\alpha$  ChIP-seq data also revealed that ER binds near the *Gata3* gene in a distal enhancer, also confirmed by ChIP qPCR, suggesting that *Gata3* is a target of ER in the normal mammary gland. Furthermore, we showed that *Gata3* is a direct target for ER $\alpha$  through down regulation after acute estradiol treatment. Our results suggest that acute treatment with estradiol represses *Gata3* gene expression leading to expansion of a de-differentiated epithelial cell population in the mammary duct. Our study also identified that estradiol-induced down regulation of *Gata3* was associated with repression of its target genes such as *Foxa1* and *Ccnd1*. It has been also shown that GATA3 is required for CCND1 expression [78]. In addition, our data suggest that *Foxa1* is involved with ER $\alpha$  binding in the normal mouse mammary gland, since motif analysis of ER $\alpha$  binding regions in the normal mammary gland showed *Foxa1* motif enrichment. Studies have shown that FOXA1 acts as a pioneer factor for ER binding in the distal enhancer sites in breast cancer cells [26, 29]. Our findings also support the notion that FOXA1 is not only involved in ER binding of breast cancer cells but also involved in ER binding in the normal mouse mammary gland. Studies have shown that the majority of ER $\alpha$  binding sites are located in the distal enhancer sites in breast cancer cells, similar to our results from the normal mammary gland. Indeed, it has also been shown that distal enhancer sites are known to interact with transcriptional complexes located near gene through DNA looping [41, 79]. Thus it is possible that ER binds distal enhancer regions and induces its target gene transcription through chromatin looping.

In conclusion, our study offers identification of ER $\alpha$  binding events across the genome under normal physiological conditions in the developing mouse mammary gland and provides a useful dataset to allow further study of estrogen signaling through its receptor. Furthermore, our findings identify cis-regulatory factors that cooperate in ER $\alpha$ -mediated control of gene expression in the normal mammary gland.

## Supporting information

**S1 Fig. Cross-correlation quality assessment of ERChIP-seq.** The blue dotted line indicates the location of the phantom peak (read length) and the red dotted lines show the library

fragment length. NSC-Normalized strand cross-correlation, RSC-Relative strand cross-correlation.

(PPTX)

**S2 Fig. Data quality evaluation of mRNA-seq.** (A) Principal component analysis showing a separation between control and E2 treatment. (B) Clustering of RNA-seq samples using Euclidean distance on normalized and log-transformed read counts.

(PPTX)

**S1 Table. List of primers used in ChIP-qPCR.**

(XLSX)

**S2 Table. Details of ER $\alpha$  ChIP-seq and RNA-seq which includes read length, total number of reads and uniquely mapped reads.**

(XLSX)

**S3 Table. List of proximal and distal motifs in ER $\alpha$  ChIP-seq.**

(XLSX)

**S4 Table. Motif enrichment analysis by HOMER.**

(XLSX)

**S5 Table. Differentially regulated genes by E2 treatment.**

(XLSX)

**S6 Table. Gene ontology terms for genes induced and repressed after 2 hours of estradiol treatment.**

(XLSX)

**S7 Table. List of direct target genes.**

(XLSX)

**S8 Table. Gene ontology terms for targetome.**

(XLSX)

## Acknowledgments

This project was supported by the Genomic and RNA Profiling Core at Baylor College of Medicine and the expert assistance of the core director, Dr. Lisa D. White, Ph.D.

## Author Contributions

**Conceptualization:** Murugesan Palaniappan.

**Data curation:** Murugesan Palaniappan, Cristian Coarfa.

**Formal analysis:** Murugesan Palaniappan, Sandra L. Grimm, Yuanxin Xi, Zheng Xia, Wei Li, Cristian Coarfa.

**Investigation:** Murugesan Palaniappan.

**Methodology:** Murugesan Palaniappan, Loc Nguyen.

**Project administration:** Murugesan Palaniappan.

**Supervision:** Murugesan Palaniappan.

**Validation:** Murugesan Palaniappan.

**Writing – original draft:** Murugesan Palaniappan.

**Writing – review & editing:** Murugesan Palaniappan.

## References

1. Hennighausen L, Robinson GW. Signaling pathways in mammary gland development. *Dev Cell*. 2001; 1(4):467–75. Epub 2001/11/13. PMID: [11703938](#).
2. Brisken C, O'Malley B. Hormone action in the mammary gland. *Cold Spring Harb Perspect Biol*. 2010; 2(12):a003178. Epub 2010/08/27. <https://doi.org/10.1101/cshperspect.a003178> PMID: [20739412](#); PubMed Central PMCID: [PMC2982168](#).
3. Siersbaek R, Kumar S, Carroll JS. Signaling pathways and steroid receptors modulating estrogen receptor alpha function in breast cancer. *Genes Dev*. 2018; 32(17–18):1141–54. Epub 2018/09/06. <https://doi.org/10.1101/gad.316646.118> PMID: [30181360](#); PubMed Central PMCID: [PMC6120708](#).
4. Palaniappan M, Edwards D, Creighton CJ, Medina D, Conneely OM. Reprogramming of the estrogen responsive transcriptome contributes to tamoxifen-dependent protection against tumorigenesis in the p53 null mammary epithelial cells. *PLoS One*. 2018; 13(3):e0194913. Epub 2018/03/29. <https://doi.org/10.1371/journal.pone.0194913> PMID: [29590203](#); PubMed Central PMCID: [PMC5874056](#).
5. Nilsson S, Makela S, Treuter E, Tujague M, Thomsen J, Andersson G, et al. Mechanisms of estrogen action. *Physiol Rev*. 2001; 81(4):1535–65. Epub 2001/10/03. <https://doi.org/10.1152/physrev.2001.81.4.1535> PMID: [11581496](#).
6. Korach KS, Couse JF, Curtis SW, Washburn TF, Lindzey J, Kimbro KS, et al. Estrogen receptor gene disruption: molecular characterization and experimental and clinical phenotypes. *Recent Prog Horm Res*. 1996; 51:159–86; discussion 86–8. Epub 1996/01/01. PMID: [8701078](#).
7. Bocchinfuso WP, Lindzey JK, Hewitt SC, Clark JA, Myers PH, Cooper R, et al. Induction of mammary gland development in estrogen receptor-alpha knockout mice. *Endocrinology*. 2000; 141(8):2982–94. Epub 2000/08/05. <https://doi.org/10.1210/endo.141.8.7609> PMID: [10919287](#).
8. Feng Y, Manka D, Wagner KU, Khan SA. Estrogen receptor-alpha expression in the mammary epithelium is required for ductal and alveolar morphogenesis in mice. *Proc Natl Acad Sci U S A*. 2007; 104(37):14718–23. Epub 2007/09/06. <https://doi.org/10.1073/pnas.0706933104> PMID: [17785410](#); PubMed Central PMCID: [PMC1976199](#).
9. Dall GV, Hawthorne S, Seyed-Razavi Y, Vieusseux J, Wu W, Gustafsson JA, et al. Estrogen receptor subtypes dictate the proliferative nature of the mammary gland. *J Endocrinol*. 2018; 237(3):323–36. Epub 2018/04/11. <https://doi.org/10.1530/JOE-17-0582> PMID: [29636363](#).
10. Echeverria PC, Picard D. Molecular chaperones, essential partners of steroid hormone receptors for activity and mobility. *Biochim Biophys Acta*. 2010; 1803(6):641–9. Epub 2009/12/17. <https://doi.org/10.1016/j.bbamcr.2009.11.012> PMID: [20006655](#).
11. Yi P, Wang Z, Feng Q, Chou CK, Pintilie GD, Shen H, et al. Structural and Functional Impacts of ER Coactivator Sequential Recruitment. *Mol Cell*. 2017; 67(5):733–43 e4. Epub 2017/08/29. <https://doi.org/10.1016/j.molcel.2017.07.026> PMID: [28844863](#); PubMed Central PMCID: [PMC5657569](#).
12. Spencer TE, Jenster G, Burcin MM, Allis CD, Zhou J, Mizzen CA, et al. Steroid receptor coactivator-1 is a histone acetyltransferase. *Nature*. 1997; 389(6647):194–8. Epub 1997/09/20. <https://doi.org/10.1038/38304> PMID: [9296499](#).
13. Lanz RB, McKenna NJ, Onate SA, Albrecht U, Wong J, Tsai SY, et al. A steroid receptor coactivator, SRA, functions as an RNA and is present in an SRC-1 complex. *Cell*. 1999; 97(1):17–27. Epub 1999/04/13. [https://doi.org/10.1016/s0092-8674\(00\)80711-4](https://doi.org/10.1016/s0092-8674(00)80711-4) PMID: [10199399](#).
14. Murakami S, Nagari A, Kraus WL. Dynamic assembly and activation of estrogen receptor alpha enhancers through coregulator switching. *Genes Dev*. 2017; 31(15):1535–48. Epub 2017/09/10. <https://doi.org/10.1101/gad.302182.117> PMID: [28887413](#); PubMed Central PMCID: [PMC5630019](#).
15. Macias H, Hinck L. Mammary gland development. *Wiley Interdiscip Rev Dev Biol*. 2012; 1(4):533–57. Epub 2012/07/31. <https://doi.org/10.1002/wdev.35> PMID: [22844349](#); PubMed Central PMCID: [PMC3404495](#).
16. Mallepell S, Krust A, Chambon P, Brisken C. Paracrine signaling through the epithelial estrogen receptor alpha is required for proliferation and morphogenesis in the mammary gland. *Proc Natl Acad Sci U S A*. 2006; 103(7):2196–201. Epub 2006/02/03. <https://doi.org/10.1073/pnas.0510974103> PMID: [16452162](#); PubMed Central PMCID: [PMC1413744](#).
17. Mueller SO, Clark JA, Myers PH, Korach KS. Mammary gland development in adult mice requires epithelial and stromal estrogen receptor alpha. *Endocrinology*. 2002; 143(6):2357–65. Epub 2002/05/22. <https://doi.org/10.1210/endo.143.6.8836> PMID: [12021201](#).



18. Ciarloni L, Mallepell S, Briskin C. Amphiregulin is an essential mediator of estrogen receptor alpha function in mammary gland development. *Proc Natl Acad Sci U S A*. 2007; 104(13):5455–60. Epub 2007/03/21. <https://doi.org/10.1073/pnas.0611647104> PMID: 17369357; PubMed Central PMCID: PMC1838509.
19. Sisto M, Lorusso L, Ingravallo G, Lisi S. Exocrine Gland Morphogenesis: Insights into the Role of Amphiregulin from Development to Disease. *Arch Immunol Ther Exp (Warsz)*. 2017; 65(6):477–99. Epub 2017/06/09. <https://doi.org/10.1007/s00005-017-0478-2> PMID: 28593345.
20. Wiseman BS, Werb Z. Stromal effects on mammary gland development and breast cancer. *Science*. 2002; 296(5570):1046–9. Epub 2002/05/11. <https://doi.org/10.1126/science.1067431> PMID: 12004111; PubMed Central PMCID: PMC2788989.
21. Carroll JS, Meyer CA, Song J, Li W, Geistlinger TR, Eeckhoutte J, et al. Genome-wide analysis of estrogen receptor binding sites. *Nat Genet*. 2006; 38(11):1289–97. Epub 2006/10/03. <https://doi.org/10.1038/ng1901> PMID: 17013392.
22. Lin CY, Vega VB, Thomsen JS, Zhang T, Kong SL, Xie M, et al. Whole-genome cartography of estrogen receptor alpha binding sites. *PLoS Genet*. 2007; 3(6):e87. Epub 2007/06/05. <https://doi.org/10.1371/journal.pgen.0030087> PMID: 17542648; PubMed Central PMCID: PMC1885282.
23. Welboren WJ, van Driel MA, Janssen-Megens EM, van Heeringen SJ, Sweep FC, Span PN, et al. ChIP-Seq of ERalpha and RNA polymerase II defines genes differentially responding to ligands. *EMBO J*. 2009; 28(10):1418–28. Epub 2009/04/03. <https://doi.org/10.1038/emboj.2009.88> PMID: 19339991; PubMed Central PMCID: PMC2688537.
24. Ross-Innes CS, Stark R, Holmes KA, Schmidt D, Spyrou C, Russell R, et al. Cooperative interaction between retinoic acid receptor-alpha and estrogen receptor in breast cancer. *Genes Dev*. 2010; 24(2):171–82. Epub 2010/01/19. <https://doi.org/10.1101/gad.552910> PMID: 20080953; PubMed Central PMCID: PMC2807352.
25. Stender JD, Kim K, Charn TH, Komm B, Chang KC, Kraus WL, et al. Genome-wide analysis of estrogen receptor alpha DNA binding and tethering mechanisms identifies Runx1 as a novel tethering factor in receptor-mediated transcriptional activation. *Mol Cell Biol*. 2010; 30(16):3943–55. Epub 2010/06/16. <https://doi.org/10.1128/MCB.00118-10> PMID: 20547749; PubMed Central PMCID: PMC2916448.
26. Franco HL, Nagari A, Kraus WL. TNFalpha signaling exposes latent estrogen receptor binding sites to alter the breast cancer cell transcriptome. *Mol Cell*. 2015; 58(1):21–34. Epub 2015/03/11. <https://doi.org/10.1016/j.molcel.2015.02.001> PMID: 25752574; PubMed Central PMCID: PMC4385449.
27. Carroll JS, Liu XS, Brodsky AS, Li W, Meyer CA, Szary AJ, et al. Chromosome-wide mapping of estrogen receptor binding reveals long-range regulation requiring the forkhead protein FoxA1. *Cell*. 2005; 122(1):33–43. Epub 2005/07/13. <https://doi.org/10.1016/j.cell.2005.05.008> PMID: 16009131.
28. Lupien M, Eeckhoutte J, Meyer CA, Wang Q, Zhang Y, Li W, et al. FoxA1 translates epigenetic signatures into enhancer-driven lineage-specific transcription. *Cell*. 2008; 132(6):958–70. Epub 2008/03/25. <https://doi.org/10.1016/j.cell.2008.01.018> PMID: 18358809; PubMed Central PMCID: PMC2323438.
29. Hurtado A, Holmes KA, Ross-Innes CS, Schmidt D, Carroll JS. FOXA1 is a key determinant of estrogen receptor function and endocrine response. *Nat Genet*. 2011; 43(1):27–33. Epub 2010/12/15. <https://doi.org/10.1038/ng.730> PMID: 21151129; PubMed Central PMCID: PMC3024537.
30. Magnani L, Ballantyne EB, Zhang X, Lupien M. PBX1 genomic pioneer function drives ERalpha signaling underlying progression in breast cancer. *PLoS Genet*. 2011; 7(11):e1002368. Epub 2011/11/30. <https://doi.org/10.1371/journal.pgen.1002368> PMID: 22125492; PubMed Central PMCID: PMC3219601.
31. Theodorou V, Stark R, Menon S, Carroll JS. GATA3 acts upstream of FOXA1 in mediating ESR1 binding by shaping enhancer accessibility. *Genome Res*. 2013; 23(1):12–22. Epub 2012/11/23. <https://doi.org/10.1101/gr.139469.112> PMID: 23172872; PubMed Central PMCID: PMC3530671.
32. Ross-Innes CS, Stark R, Teschendorff AE, Holmes KA, Ali HR, Dunning MJ, et al. Differential oestrogen receptor binding is associated with clinical outcome in breast cancer. *Nature*. 2012; 481(7381):389–93. Epub 2012/01/06. <https://doi.org/10.1038/nature10730> PMID: 22217937; PubMed Central PMCID: PMC3272464.
33. Nautiyal J, Steel JH, Mane MR, Oduwole O, Poliandri A, Alexi X, et al. The transcriptional co-factor RIP140 regulates mammary gland development by promoting the generation of key mitogenic signals. *Development*. 2013; 140(5):1079–89. Epub 2013/02/14. <https://doi.org/10.1242/dev.085720> PMID: 23404106; PubMed Central PMCID: PMC3583043.
34. Goecks J, Nekrutenko A, Taylor J. Galaxy: a comprehensive approach for supporting accessible, reproducible, and transparent computational research in the life sciences. *Genome Biol*. 2010; 11(8):R86. Epub 2010/08/27. <https://doi.org/10.1186/gb-2010-11-8-r86> PMID: 20738864; PubMed Central PMCID: PMC2945788.

35. Blankenberg D, Von Kuster G, Coraor N, Ananda G, Lazarus R, Mangan M, et al. Galaxy: a web-based genome analysis tool for experimentalists. *Curr Protoc Mol Biol.* 2010;Chapter 19:Unit 19 0 1–21. Epub 2010/01/14. <https://doi.org/10.1002/0471142727.mb1910s89> PMID: 20069535; PubMed Central PMCID: PMC4264107.
36. Giardine B, Riemer C, Hardison RC, Burhans R, Elnitski L, Shah P, et al. Galaxy: a platform for interactive large-scale genome analysis. *Genome Res.* 2005; 15(10):1451–5. Epub 2005/09/20. <https://doi.org/10.1101/gr.4086505> PMID: 16169926; PubMed Central PMCID: PMC1240089.
37. Marinov GK, Kundaje A, Park PJ, Wold BJ. Large-scale quality analysis of published ChIP-seq data. *G3 (Bethesda).* 2014; 4(2):209–23. Epub 2013/12/19. <https://doi.org/10.1534/g3.113.008680> PMID: 24347632; PubMed Central PMCID: PMC3931556.
38. Liu T, Ortiz JA, Taing L, Meyer CA, Lee B, Zhang Y, et al. Cistrome: an integrative platform for transcriptional regulation studies. *Genome Biol.* 2011; 12(8):R83. Epub 2011/08/24. <https://doi.org/10.1186/gb-2011-12-8-r83> PMID: 21859476; PubMed Central PMCID: PMC3245621.
39. Heinz S, Benner C, Spann N, Bertolino E, Lin YC, Laslo P, et al. Simple combinations of lineage-determining transcription factors prime cis-regulatory elements required for macrophage and B cell identities. *Mol Cell.* 2010; 38(4):576–89. Epub 2010/06/02. <https://doi.org/10.1016/j.molcel.2010.05.004> PMID: 20513432; PubMed Central PMCID: PMC2898526.
40. Dennis G Jr., Sherman BT, Hosack DA, Yang J, Gao W, Lane HC, et al. DAVID: Database for Annotation, Visualization, and Integrated Discovery. *Genome Biol.* 2003; 4(5):P3. Epub 2003/05/08. PMID: 12734009.
41. Fullwood MJ, Liu MH, Pan YF, Liu J, Xu H, Mohamed YB, et al. An oestrogen-receptor- $\alpha$ -bound human chromatin interactome. *Nature.* 2009; 462(7269):58–64. Epub 2009/11/06. <https://doi.org/10.1038/nature08497> PMID: 19890323; PubMed Central PMCID: PMC2774924.
42. Li B, Dewey CN. RSEM: accurate transcript quantification from RNA-Seq data with or without a reference genome. *BMC Bioinformatics.* 2011; 12:323. Epub 2011/08/06. <https://doi.org/10.1186/1471-2105-12-323> PMID: 21816040; PubMed Central PMCID: PMC3163565.
43. Robinson MD, McCarthy DJ, Smyth GK. edgeR: a Bioconductor package for differential expression analysis of digital gene expression data. *Bioinformatics.* 2010; 26(1):139–40. Epub 2009/11/17. <https://doi.org/10.1093/bioinformatics/btp616> PMID: 19910308; PubMed Central PMCID: PMC2796818.
44. Durchdewald M, Guinea-Viniegra J, Haag D, Riehl A, Lichter P, Hahn M, et al. Podoplanin is a novel fos target gene in skin carcinogenesis. *Cancer Res.* 2008; 68(17):6877–83. Epub 2008/09/02. <https://doi.org/10.1158/0008-5472.CAN-08-0299> PMID: 18757399.
45. Miyamoto-Sato E, Fujimori S, Ishizaka M, Hirai N, Masuoka K, Saito R, et al. A comprehensive resource of interacting protein regions for refining human transcription factor networks. *PLoS One.* 2010; 5(2): e9289. Epub 2010/03/03. <https://doi.org/10.1371/journal.pone.0009289> PMID: 20195357; PubMed Central PMCID: PMC2827538.
46. Lain AR, Creighton CJ, Conneely OM. Research resource: progesterone receptor targetome underlying mammary gland branching morphogenesis. *Mol Endocrinol.* 2013; 27(10):1743–61. Epub 2013/08/28. <https://doi.org/10.1210/me.2013-1144> PMID: 23979845; PubMed Central PMCID: PMC3787126.
47. Usary J, Llaca V, Karaca G, Presswala S, Karaca M, He X, et al. Mutation of GATA3 in human breast tumors. *Oncogene.* 2004; 23(46):7669–78. Epub 2004/09/14. <https://doi.org/10.1038/sj.onc.1207966> PMID: 15361840.
48. Kouros-Mehr H, Slorach EM, Sternlicht MD, Werb Z. GATA-3 maintains the differentiation of the luminal cell fate in the mammary gland. *Cell.* 2006; 127(5):1041–55. Epub 2006/11/30. <https://doi.org/10.1016/j.cell.2006.09.048> PMID: 17129787; PubMed Central PMCID: PMC2646406.
49. Asselin-Labat ML, Sutherland KD, Barker H, Thomas R, Shackleton M, Forrest NC, et al. Gata-3 is an essential regulator of mammary-gland morphogenesis and luminal-cell differentiation. *Nat Cell Biol.* 2007; 9(2):201–9. Epub 2006/12/26. <https://doi.org/10.1038/ncb1530> PMID: 17187062.
50. Arnold JM, Choong DY, Thompson ER, Waddell N, Lindeman GJ, Visvader JE, et al. Frequent somatic mutations of GATA3 in non-BRCA1/BRCA2 familial breast tumors, but not in BRCA1-, BRCA2- or sporadic breast tumors. *Breast Cancer Res Treat.* 2010; 119(2):491–6. Epub 2009/02/04. <https://doi.org/10.1007/s10549-008-0269-x> PMID: 19189213.
51. Garcia-Closas M, Troester MA, Qi Y, Langerod A, Yeager M, Lissowska J, et al. Common genetic variation in GATA-binding protein 3 and differential susceptibility to breast cancer by estrogen receptor  $\alpha$  tumor status. *Cancer Epidemiol Biomarkers Prev.* 2007; 16(11):2269–75. Epub 2007/11/17. <https://doi.org/10.1158/1055-9965.EPI-07-0449> PMID: 18006915.
52. Chanock SJ, Burdett L, Yeager M, Llaca V, Langerod A, Presswala S, et al. Somatic sequence alterations in twenty-one genes selected by expression profile analysis of breast carcinomas. *Breast Cancer Res.* 2007; 9(1):R5. Epub 2007/01/17. <https://doi.org/10.1186/bcr1637> PMID: 17224074; PubMed Central PMCID: PMC1851401.

53. Cakir A, Isik Gonul I, Ekinci O, Cetin B, Benekli M, Uluoglu O. GATA3 expression and its relationship with clinicopathological parameters in invasive breast carcinomas. *Pathol Res Pract*. 2017; 213(3):227–34. Epub 2017/02/22. <https://doi.org/10.1016/j.prp.2016.12.010> PMID: 28215639.
54. Asch-Kendrick R, Cimino-Mathews A. The role of GATA3 in breast carcinomas: a review. *Hum Pathol*. 2016; 48:37–47. Epub 2016/01/17. <https://doi.org/10.1016/j.humpath.2015.09.035> PMID: 26772397.
55. Hurtado A, Holmes KA, Geistlinger TR, Hutcheson IR, Nicholson RI, Brown M, et al. Regulation of ERBB2 by oestrogen receptor-PAX2 determines response to tamoxifen. *Nature*. 2008; 456(7222):663–6. Epub 2008/11/14. <https://doi.org/10.1038/nature07483> PMID: 19005469; PubMed Central PMCID: PMC2920208.
56. Caizzi L, Ferrero G, Cutrupi S, Cordero F, Ballare C, Miano V, et al. Genome-wide activity of unliganded estrogen receptor- $\alpha$  in breast cancer cells. *Proc Natl Acad Sci U S A*. 2014; 111(13):4892–7. Epub 2014/03/19. <https://doi.org/10.1073/pnas.1315445111> PMID: 24639548; PubMed Central PMCID: PMC3977241.
57. Hewitt SC, Li L, Grimm SA, Chen Y, Liu L, Li Y, et al. Research resource: whole-genome estrogen receptor  $\alpha$  binding in mouse uterine tissue revealed by ChIP-seq. *Mol Endocrinol*. 2012; 26(5):887–98. Epub 2012/03/27. <https://doi.org/10.1210/me.2011-1311> PMID: 22446102; PubMed Central PMCID: PMC3355558.
58. Bernardo GM, Lozada KL, Miedler JD, Harburg G, Hewitt SC, Mosley JD, et al. FOXA1 is an essential determinant of ER $\alpha$  expression and mammary ductal morphogenesis. *Development*. 2010; 137(12):2045–54. Epub 2010/05/27. <https://doi.org/10.1242/dev.043299> PMID: 20501593; PubMed Central PMCID: PMC2875844.
59. Mulac-Jericevic B, Lydon JP, DeMayo FJ, Conneely OM. Defective mammary gland morphogenesis in mice lacking the progesterone receptor B isoform. *Proceedings of the National Academy of Sciences of the United States of America*. 2003; 100(17):9744–9. Epub 2003/08/05. <https://doi.org/10.1073/pnas.1732707100> PMID: 12897242; PubMed Central PMCID: PMC187836.
60. Conneely OM, Mulac-Jericevic B, Arnett-Mansfield R. Progesterone signaling in mammary gland development. *Ernst Schering Found Symp Proc*. 2007;(1):45–54. Epub 2008/06/11. PMID: 18543434.
61. Mulac-Jericevic B, Mullinax RA, DeMayo FJ, Lydon JP, Conneely OM. Subgroup of reproductive functions of progesterone mediated by progesterone receptor-B isoform. *Science*. 2000; 289(5485):1751–4. Epub 2000/09/08. <https://doi.org/10.1126/science.289.5485.1751> PMID: 10976068.
62. Dupont S, Krust A, Gansmuller A, Dierich A, Chambon P, Mark M. Effect of single and compound knockouts of estrogen receptors  $\alpha$  (ER $\alpha$ ) and  $\beta$  (ER $\beta$ ) on mouse reproductive phenotypes. *Development*. 2000; 127(19):4277–91. Epub 2000/09/08. PMID: 10976058.
63. Ghosh MG, Thompson DA, Weigel RJ. PDZK1 and GREB1 are estrogen-regulated genes expressed in hormone-responsive breast cancer. *Cancer Res*. 2000; 60(22):6367–75. Epub 2000/12/05. PMID: 11103799.
64. Carroll JS, Brown M. Estrogen receptor target gene: an evolving concept. *Mol Endocrinol*. 2006; 20(8):1707–14. Epub 2006/01/07. <https://doi.org/10.1210/me.2005-0334> PMID: 16396959.
65. Rae JM, Johnson MD, Scheys JO, Cordero KE, Larios JM, Lippman ME. GREB 1 is a critical regulator of hormone dependent breast cancer growth. *Breast Cancer Res Treat*. 2005; 92(2):141–9. Epub 2005/06/30. <https://doi.org/10.1007/s10549-005-1483-4> PMID: 15986123.
66. Sun J, Nawaz Z, Slingerland JM. Long-range activation of GREB1 by estrogen receptor via three distal consensus estrogen-responsive elements in breast cancer cells. *Mol Endocrinol*. 2007; 21(11):2651–62. Epub 2007/08/02. <https://doi.org/10.1210/me.2007-0082> PMID: 17666587.
67. Deschenes J, Bourdeau V, White JH, Mader S. Regulation of GREB1 transcription by estrogen receptor  $\alpha$  through a multipartite enhancer spread over 20 kb of upstream flanking sequences. *J Biol Chem*. 2007; 282(24):17335–9. Epub 2007/04/28. <https://doi.org/10.1074/jbc.C700030200> PMID: 17463000.
68. Carroll JS, Hickey TE, Tarulli GA, Williams M, Tilley WD. Deciphering the divergent roles of progestogens in breast cancer. *Nat Rev Cancer*. 2017; 17(1):54–64. Epub 2016/11/26. <https://doi.org/10.1038/nrc.2016.116> PMID: 27885264.
69. Stingl J. Estrogen and progesterone in normal mammary gland development and in cancer. *Horm Cancer*. 2011; 2(2):85–90. Epub 2011/07/16. <https://doi.org/10.1007/s12672-010-0055-1> PMID: 21761331.
70. Karin M, Liu Z, Zandi E. AP-1 function and regulation. *Curr Opin Cell Biol*. 1997; 9(2):240–6. Epub 1997/04/01. PMID: 9069263.
71. Zhao GQ, Liaw L, Hogan BL. Bone morphogenetic protein 8A plays a role in the maintenance of spermatogenesis and the integrity of the epididymis. *Development*. 1998; 125(6):1103–12. Epub 1998/05/09. PMID: 9463357.

72. Chung D, Gao F, Jegga AG, Das SK. Estrogen mediated epithelial proliferation in the uterus is directed by stromal Fgf10 and Bmp8a. *Mol Cell Endocrinol*. 2015; 400:48–60. Epub 2014/12/03. <https://doi.org/10.1016/j.mce.2014.11.002> PMID: 25451979; PubMed Central PMCID: PMC4751583.
73. Perou CM, Sorlie T, Eisen MB, van de Rijn M, Jeffrey SS, Rees CA, et al. Molecular portraits of human breast tumours. *Nature*. 2000; 406(6797):747–52. Epub 2000/08/30. <https://doi.org/10.1038/35021093> PMID: 10963602.
74. Sotiriou C, Neo SY, McShane LM, Korn EL, Long PM, Jazaeri A, et al. Breast cancer classification and prognosis based on gene expression profiles from a population-based study. *Proc Natl Acad Sci U S A*. 2003; 100(18):10393–8. Epub 2003/08/15. <https://doi.org/10.1073/pnas.1732912100> PMID: 12917485; PubMed Central PMCID: PMC193572.
75. Comprehensive molecular portraits of human breast tumours. *Nature*. 2012; 490(7418):61–70. Epub 2012/09/25. <https://doi.org/10.1038/nature11412> PMID: 23000897; PubMed Central PMCID: PMC3465532.
76. Kouros-Mehr H, Werb Z. Candidate regulators of mammary branching morphogenesis identified by genome-wide transcript analysis. *Dev Dyn*. 2006; 235(12):3404–12. Epub 2006/10/14. <https://doi.org/10.1002/dvdy.20978> PMID: 17039550; PubMed Central PMCID: PMC2730892.
77. Grober OM, Mutarelli M, Giurato G, Ravo M, Cicatiello L, De Filippo MR, et al. Global analysis of estrogen receptor beta binding to breast cancer cell genome reveals an extensive interplay with estrogen receptor alpha for target gene regulation. *BMC Genomics*. 2011; 12:36. Epub 2011/01/18. <https://doi.org/10.1186/1471-2164-12-36> PMID: 21235772; PubMed Central PMCID: PMC3025958.
78. Shan L, Li X, Liu L, Ding X, Wang Q, Zheng Y, et al. GATA3 cooperates with PARP1 to regulate CCND1 transcription through modulating histone H1 incorporation. *Oncogene*. 2014; 33(24):3205–16. Epub 2013/07/16. <https://doi.org/10.1038/onc.2013.270> PMID: 23851505.
79. Panigrahi AK, Foulds CE, Lanz RB, Hamilton RA, Yi P, Lonard DM, et al. SRC-3 Coactivator Governs Dynamic Estrogen-Induced Chromatin Looping Interactions during Transcription. *Mol Cell*. 2018; 70(4):679–94 e7. Epub 2018/05/19. <https://doi.org/10.1016/j.molcel.2018.04.014> PMID: 29775582; PubMed Central PMCID: PMC5966282.